EFDA–JET–PR(13)02

P. Devynck, C. Giroud, P. Jacquet, M. Lehnen, E. Lerche, G. Maddison,
G.F. Matthews, M-L. Mayoral, R. Neu, M.F. Stamp, D. Van Eester
and JET EFDA contributors

The Scaling of Radiated Power in the Bulk Plasma of JET

The Scaling of Radiated Power in the Bulk Plasma of JET

P. Devynck[1], C. Giroud[2], P. Jacquet[2], M. Lehnen[3], E. Lerche[4], G. Maddison[2], G.F. Matthews[2], M-L. Mayoral[2], R. Neu[5], M.F. Stamp[2], D. Van Eester[4] and JET EFDA contributors*

JET-EFDA, Culham Science Centre, OX14 3DB, Abingdon, UK

[1]CEA-IRFM F-13108 Saint-Paul-lez-Durance, France
[2]EURATOM-CCFE Fusion Association, Culham Science Centre, OX14 3DB, Abingdon, OXON, UK
[3]Institut für Energie-und-Klimaforschung-Plasmaphysik, forschungzentrum Jülich, Germany
[4]Association EURATOM-Belgian state, ERM-KRS, Brussels, Belgium
[5]Max-Planck-institut für Plasmaphysik, Euratom Association, D-85748 Garching, Germany
** See annex of F. Romanelli et al, "Overview of JET Results", (24th IAEA Fusion Energy Conference, San Diego, USA (2012)).*

Preprint of Paper to be submitted for publication in
Nuclear Fusion

ABSTRACT

We show that in all JET plasmas, in JET ITER-like Wall (ILW) or Carbon Environment, in Limiter or Divertor mode, Ohmic, H or L mode, the bulk radiated power is a function of the line density, Z_{eff} and a parameter βr that contains all the atomic physics of the radiating impurities. The values taken by br are imposed by the nature of the wall components and the type of plasma diverted or limited.

In ILW no strong dependence on the confinement (H or L mode) and on the spatial distribution of the radiation is found. In ILW this parameter takes values around 11 while in Carbon environment it is around 1. The difference between the two configurations shows that the species polluting the bulk are much more radiative in the case of ILW than in the case of Carbon environment. Moreover, the parameter βr measured in a statistical way is in fact found to describe the discharge at all times. Its temporal evolution can be used to monitor changes of the composition of the discharge impurities. The knowledge of br in a discharge allows calculating what range of densities or Z_{eff} must not be reached to avoid a radiative collapse of the plasma. Finally, we find that βr can characterize the radiative efficiency of the impurities in other machines.

INTRODUCTION

Nowadays, tungsten is investigated as the preferred future material for tokamak divertors as its use solves several problems:

The first one is that fuel retention is minimized by the use of tungsten [1,2]. Another positive aspect of Tungsten is that it is eroded at higher plasma temperatures than Carbon [3]. It is at the moment being tested in other tokamaks [4] and is envisaged as the prime material for the Divertor of ITER. However, apart from these qualities there are some difficulties to operate machines with this type of high Z material. This is because high Z elements can radiate in the plasma core [5,6]. The presence of radiation in the centre of the discharge is now a major concern for these machines and important efforts are being made at the moment to identify the radiating impurities in the core and estimate their amount.

Spectrometers used for this purpose cover only lines or bundle of lines of these high Z impurities along limited lines of sight and it is difficult from these measurements to deduce concentrations of impurities. This can be done with the help of radiation models that must calculate the ionization equilibrium and that must include also the transport of the impurities. For high Z elements, these models are in the best of cases only approximate. The case of Tungsten is particularly difficult as a lot of the coefficients of radiative transitions of the highest ionization states are at the moment unknown.

As a result any information that can be gained about the radiative efficiency of the impurities polluting the bulk can be useful. This paper is a step in that direction. We analyse data from JET in its ITER-like Wall (ILW) configuration [7] with Tungsten Divertor and Beryllium walls and compare it with similar data from the Carbon environment.

We show that even global parameters can carry useful information about the type of impurities

polluting the bulk of the discharge. In order to do this, we establish experimentally the relationship between the bulk radiated power, the effective charge Z_{eff} of the discharge and the line density. We deduce from this relationship a parameter br that characterizes how much power is radiated in the bulk relatively to Z_{eff} and the density. The value taken by this parameter is found to be almost the same in diverted ILW discharges and has a lesser value in the Carbon environment. The high value of the br parameter in ILW points towards high Z impurities in the bulk that is very efficient at radiating there. As a difference, the low value of br in Carbon environment indicates the presence of low Z impurities poorly radiating in the bulk. As a result, by measuring βr, it is possible to have an idea of the type of impurities radiating in the bulk of the discharge.

As this study is experimental, we start by introducing the database that has been analysed in section 1. We then deal with the selection of the data relative to the stationarity problem in section 2. In section 3, we describe the procedure that is used to filter the ELMS in order to analyse only quiet phases of the plasma. In section 4 we introduce the relationship between $Prad_{bulk}$, Z_{eff} and N_e. We also give the meaning of the βr value that is deduced from the scaling. In section 5 we present the results obtained for the ILW with shots in L mode both in Divertor and Limiter configuration. We also discuss the results obtained by comparing shots in L and H mode for the ILW. In section 6, we discuss the effect of different types of additional heating on the value of βr. In section 7, we switch to the Carbon environment and we show that the scaling found in ILW also apply to the bulk of these discharge and yields a βr parameter at least 10 times smaller than in ILW. In section 8, we discuss the influence of the Divertor radiation on the scaling and we compare our results with the multi-machine scaling [8] that was found to describe the link between total radiated power and Z_{eff} in Carbon environment machines. In section 9, we discuss how to compare the radiative efficiency of different discharges using the βr parameter. For this purpose we introduce the notion of the "equivalent" discharge that is a simplified discharge with the same macroscopic radiative properties than the real one. In section 10, we discuss the operational limits introduced by the high values of βr in ILW. This translates in a limited range of Z_{eff} values to operate the plasma to avoid a disruption triggered by a radiated fraction equal to one in the centre of the plasma. In section 11, we show that the relationship between $Prad_{bulk}$, Z_{eff} and N_e established in a statistical way is in fact valid at all times in the plasma. As a result, βr is a time dependent parameter whose evolution can be followed allowing studying non stationary phases of the plasma. We illustrate this by analysing a shot where the radiated power is found to increase in the bulk during the additional heating phase. Finally in section 12, we compare βr/V obtained in two machines equipped with Carbon components, Tore Supra and JET for plasmas run in limiter mode. We finish in section 13 with the conclusions.

1. DATABASE

For the phase of JET operation with the ILW, we tested the scaling law on several hundred shots in Ohmic, H or L mode of the JET database during the end of the 2011 campaign and throughout the 2012 campaign. The end of the 2011 campaign was mostly dedicated to Ohmic and L mode shots

with limited additional heating power mostly ICRH. In 2012, the main additional heating power on JET (NBI) was increased up to 25MW and powerful H mode shots were routinely obtained. For the Carbon configuration shots, we scanned randomly the database for the 2008 and 2009 campaigns. We present in the paper shots from experiments where N2 seeding was performed and shots from disruption studies that include a time window in Limiter mode. However the results presented here apply to plasmas obtained at least over a 4 year period during which many types of experiments were performed with different plasma shapes, beta values, level of additional heating, seeding of Nitrogen etc. The data were collected only on the current plateau phase. All data were re-sampled at 10 or 1 ms depending on the experiments, and collected only during additional heating phases for L and H mode discharges. Ohmic shots were also investigated and gave similar results. The phases before and after X point formation were also discriminated as the action of the Divertor on the impurities was found to be an important player for the amplitude of bulk radiation. Finally, during H mode, the problem of the identification of time windows in between ELMS had to be addressed. As this is a difficult problem that is important for the output of the analysis, we are going to detail the procedure used below.

2. STEADY STATE VERSUS QUIET PHASES

In the conventional approach for data analysis, one in general seeks steady state phases that correspond at least to a momentary equilibrium. This comes from the idea that if some parameters are changing during the measurement, the link found between various parameters may be biased or disrupted by transitory effects corresponding to the non stationarity of the processes. As a result the conventional wisdom is that any relationship established between physical quantities may be biased. If the stationary state corresponds to the most desirable state for the analysis, it is sometimes too restrictive (only a very tiny fraction of the data can be analysed) or even irrelevant because the object being studied may be by nature a dynamical object. In that case it is necessary to seek laws that are sufficiently robust to accommodate a parametric change and can therefore describe an object throughout its time evolution. As far as the plasmas of JET are concerned, we are clearly in the case where true stationarity is very seldom attained. Global parameters such as density, applied power, mean Te, plasma position, vary in time. We are going to abandon the idea that only stationary phases can be studied and include in the analysis time windows during which parametric changes occur. The validity of the analysis will be checked a-posteriori by checking the coherence of the result. For example a unique scaling law that covers non stationary time windows also describes the stationary phases that are present in the data. However some transient phenomena occurring in the plasma can be so massive and violent that they certainly will disrupt any scaling. The most obvious of them in JET are the ELMS [9] occurring in H mode and taking place at the edge of the plasma. ELMS deposit power and particles on the wall and divertor leading to large transient influxes of impurities. These will have to be filtered out and the remaining times will be used for the data analysis. The remaining times are not “stationary phases” but are quieter phases during

which a parametric study can be tried. We describe below how we can filter the ELMS to obtain these quieter phases.

3. FILTERING THE ELMS

First of all, to select the time windows, we consider that the magnetic geometry of the plasma should be fixed. This excludes from the analysis the plasma current ramp up and down phases. Apart from this, there are no more restrictions and the other plasma parameters can vary widely. Different signals can be used to filter the ELMS. They are visible on the Divertor radiated power, on probes embedded in the Divertor but also on thermography signals looking at the Divertor tiles such as QMX5 that is sampled with a very good sampling rate (100μs). The ELMS are observed on all diagnostics as large asymmetric peaks with a fast front and a slower decay. They can come in unique events or be followed by a fast succession of small crashes. They can have a pseudo periodic structure with a chaotic behaviour or in some extreme cases appear as a continuum of peaks. The difficulty is that an ELM may be just a single relaxation or a number of relaxations and the filtering should take care of this. Figure 1 displays the thermography signal of tile 5 of the Divertor. It is possible to filter the ELMS on this signal and use the quiet phases defined with it to select the time windows of the other useful signals. It is obtained for a shot with Nitrogen seeding in the machine in carbon environment. We observe in Figure 1 that the peaks are grouped in packs separated by larger time intervals. Another important observation is that the apparent "frequency" of the ELMS is changing throughout time: the frequency is decreasing with time.

To decide what an ELM is, we are going to use a technique based on the behaviour of the self correlation time function. The self correlation function of a signal writes as

$$c(\tau) = \int x(t)\, x(t+\tau)\, dt$$

x(t) being the signal at time τ, and t the lag at which the correlation coefficient is calculated. The correlation c is being calculated for all possible values of τ. The self correlation function obtained in this way is normalized to 1 at zero lag value. This calculation applied to the data of Figure 1 is plotted in Figure 2. Figure 2 shows that the self-correlation function of the signal is decreasing with τ with two slopes. The end of the first slope allows calculating the self-correlation time of the individual peaks. The second slope corresponds to the cross-correlation of the different peaks belonging to the same pack [10]. The end of the second slope allows defining a threshold time to. This is the minimum time by which 2 successive peaks must be separated to be considered as independent. In order to obtain this threshold time, the time series $\delta c = c(\tau + 1) - c(\tau)$ is calculated for all τ values. δc starts negative but increases with τ.

The value to at which δc becomes positive again defines the threshold time. Any successive peaks separated by less than to must be considered as only one structure. This routine is run not on the data itself but on a gate function. This gate function is set at 1 for time widows during which peaks are

detected on the raw signal, zero elsewhere. When two peaks are separated by less than to, the gate function is set to 1 during the time window encompassing the two peaks. At the end of the routine, the times at which the gate function is equal to zero are the "quiet" time phases of the plasma that can be used for the analysis. Figure 3 shows the final result of the filtering on the raw data. The red circles are the times outside the crash of the ELMS. During these times, the plasma is still under the influence of the crash of the ELM and has to recover so that in between the ELMS it cannot be considered as stationary. Nevertheless the parametric variation is supposed to be sufficiently slow so that an analysis can be tried. As discussed above the validity of this hypothesis will be checked a posteriori i.e. by establishing if a scaling law covering the selected data is possible or not. If most of the ELMS are observed as pseudo-periodic structures, there are shots where they form a continuum of peaks to such a point that their relaxations at the edge of the plasma can be almost considered as a turbulent process. This is observed when some massive impurity seeding is performed. We show in Figure 4 a signal corresponding to this case measured on the thermography of tile 5. In this shot at high NBI power in Carbon environment, an extremely high level of N2 was injected into the discharge. In that case the existence of quiet phases cannot really be defined; however, it is still possible to define times outside of ELM crashes. The situation is complicated by the fact that the discharge evolves from pseudo-periodic behaviour at the beginning of the N2 injection to a continuum of peaks (shown in the Figure). As a result, the correlation time of the signal changes from the start of the time series to the end of it. To take this into account, another refinement has been added to the routine: it is the possibility to split the signal in several time windows in order to calculate the self-correlation on each of these time windows thus yielding several threshold times to. This can be efficient but must be performed with caution as the self-correlation function will become very noisy when the number of data points is too much reduced. This has been done on the data of Figure 4 by splitting the time series in 2 and the result is illustrated in the same Figure.

4. GENERAL DEPENDENCE OF PRAD WITH ZEFF IN THE BULK.

The multi-machine scaling [8] established a relationship between total radiated power and Z_{eff}. In this analysis we test a similar relationship in the bulk of the plasma. This region is simpler than the Divertor one where ionisation and recycling take place. It seems also slightly more relevant as we use global parameters such as Z_{eff} and Ne that are highly weighted by the bulk of the discharge. For ILW studies, the value of Z_{eff} that is used is the one calculated from the horizontal line of sight of the Bremsstrahlung [11] that is not passing through the Divertor region. The density is the line integrated one provided by the high resolution Thomson scattering [12]. Prad in the bulk is evaluated by the bolometry with the most recent cameras (KB5) of JET [13]. In order to get the bulk radiated power, the bolometric lines of sight of the top half of the plasma are used. Each of them is projected along an horizontal direction and the volume covered by these lines of sight is stretched to fill the whole plasma volume.

The main result is that Z_{eff} is found to be a linear function of $Prad_{bulk}/Ne^2$.

$$Z_{eff} = 1 + a\ Prad_{bulk}/Ne^2 \quad (1)$$

In this expression, a is calculated by writing Pradbulk in MW and Ne in 1020 m-2. This law is found to be valid under most conditions, L mode, H mode, Ohmic, Divertor or Limiter operation and regardless of the Divertor of wall components (ILW or Carbon environment). The only condition that has to be fulfilled is that the plasma is in a "quiet phase" as defined above and that the bulk radiated power is not saturated. The only parameter that depends on experimental conditions is the parameter a in the scaling. This parameter is of course linked to the radiating properties of the impurities. To illustrate this, we can write relation 1 in the following way:

$$\beta r = 1/a = Prad_{bulk}/(Z_{eff} - 1)Ne^2 \quad (2)$$

The inverse of a characterizes the radiated power per Z_{eff} corrected from the Deuterium contribution and from the effect of the density. In the bulk plasma at least two mechanisms create radiation.

The first one is the Bremsstrahlung radiation that is very dependent on the central density. As the discharges get more and more powerful and the density is raised, this contribution may not be neglected. This radiation will give account for a good fraction of the radiation in the bulk of ITER [14]. It depends on the product of Ne^2 with Z_{eff} so that br expressed in relation 2 certainly contains the contribution of the Bremsstrahlung. The contribution of the Bremsstrahlung to the value of br will increase as $Z_{eff}/(Z_{eff} - 1)$ i.e will be maximum when Z_{eff} tends towards 1 at very high Ne values. However, we found that a unique βr value can describe series of shots where the density is scanned from low values up to the Greenwald density [15]. This indicates that the Bremsstrahlung radiation is not the dominant radiation mechanism in the shots of JET. We will neglect it in the rest of the paper.

The other contribution is the radiation produced by the impurities partially ionised in the bulk of the plasma. We suppose in the rest of the paper that this is the dominant contribution to the radiation and that the changes of the βr parameter are directly linked to this type of radiation. So βr = 1/a characterizes the efficiency of the bulk impurities to radiate; it contains all the atomic physics of the radiation and includes all the types of impurities present in the plasma, with different spatial dependencies (related to transport). Because of this, it will be probably difficult to recover through code simulation. Relation 2 implies that the plasma is self organised so that the amount of radiated power in the bulk can be described using only global parameters such as Z_{eff}, Ne and br that carries all the atomic physics of the mixture of the radiating impurities.

In order to better understand the meaning of br, we give its expression for a general case where different types of impurities with different ionisation levels are present in Deuterium plasma. Firstly, for only one type of impurity the radiated power in the bulk writes as:

$$\Pr ad_{bulk} = NeN_{imp}\, V \sum_i a_i\, b_i\, c_i\, Lt_i\ .$$

In this expression Nimp is the total impurity density, Ne the electron density, $a_i = N_i/N_{imp}$ the fraction

of impurity ions with charge z_i, $b_i = Ne_i/Ne$, the fraction of the density in the volume where the ion with charge z_i radiates and $c_i = V_i/V$ the fraction of the volume in which the same ion radiates. Lti is the radiative cooling function for the same ion with charge z_i. We suppose in this expression that the temperature Te is homogenous in the volume where the ion of charge z_i is radiating, as well as the density of impurity ions and electrons. This is only an approximation. If we extend this to different impurities we get:

$$\Pr ad_{bulk} = NeV \sum_k N_{imp}^k \sum_i a_i^k b_i^k c_i^k Lt_i^k$$

where k denotes different types of impurities. We can write the expression for Z_{eff} as:

$$Z_{eff} = 1 + \frac{1}{Ne} \sum_k N_{imp}^k \sum_i a_i^k z_i^k (z_i^k - 1)$$

if we combine these expressions with relation 2 (i.e. assuming that relation 2 holds) we find

$$\beta_r / V = \frac{\sum_k \varepsilon_{imp}^k \sum_i a_i^k b_i^k c_i^k Lt_i^k}{\sum_k \varepsilon_{imp}^k \sum_i a_i^k z_i^k (z_i^k - 1)} \quad where\ \varepsilon_{imp}^k = \frac{N_{imp}^k}{\sum_k N_{imp}^k} \tag{3}$$

We notice several things about this expression, first of all βr/V is not dimensionless, it has the dimension of Lt and can be expressed in $W.m^3$. It is proportional to the total cooling rate of the bulk discharge.

Secondly, βr/V depends on the fraction of the total volume occupied by the radiative impurities through the parameter c_i^k. This parameter depends on the temperature profile, on the transport coefficients of the impurities but also on the size of the machine. This is especially true for low Z impurities such as Carbon. For example, the volume where the Carbon ions radiate will be a narrow layer at the edge of the plasma that will not increase linearly with the plasma volume.
Another point is that there is no information in that parameter about the amount of impurities contaminating the discharge (the term N_{imp} disappeared). It depends only on their relative distribution. βr is in fact a weighted sum of radiative cooling functions divided by a dimensionless expression that is the weighted sum of the z_i^2 of the corresponding ions.

Expression 3 indicates that the most sensitive parameter to change br is the term ε^k_{imp}, the fraction (relative to the total amount of impurities) of different impurities in the discharge. If the shape of temperature and density profiles is resilient, changes in the distribution of ionisations levels for a given impurity will also affect the value of βr but probably to a lesser extent as a summation of radiative functions over many different ionisation levels varies probably less than the relative contribution of the different impurities through the term ε^k_{imp}.

Finally, in order for br to increase, the weighted sum of Lt must increase faster than the corresponding sum of z_i^2. This suggests that the dynamical range of values taken by br will be limited;

experimentally we will measure βr values comprised between 0 and 15. Values above 10 will be measured only in the case where high Z materials are expected to pollute the bulk of the discharge in ILW. We also will find that the number of values that br can take are limited. The br parameter changes little from one shot to the next but depends essentially on the type of environment, ILW or Carbon and on the type of plasma diverted or limited.

5. DETERMINATION OF BR IN JET ILW.

We show in Figure 5, the scaling obtained at the end of the 2011 campaign of JET on different series of diverted and limited shots mostly in L mode with some transitions in H mode for the diverted ones but without any ELMS. The main additional heating is ICRH waves and the applied power is limited as total applied power (Ohmic plus additional heating power) ranges between 1.4 and 6MW. The line density is varied from 0.3 to 1.2 1020 m^{-2}. The plasma current takes two values 1.95MA and 2.5MA. The data plotted in Figure 5 includes 51 shots measured over a time period covering several weeks. The data are found to follow closely relation 1 with a standard deviation of the data around the linear fit at about 0.08 for the diverted plasmas, less for the limiter ones. The slope a of the Divertor data is found to be 0.088 which sets br at 11.36. In this case, a calculation of the uncertainty of br that takes into account the standard deviation of the data around the fit gives br being bounded between 10 and 13. In Figure 5, the quality of the alignment illustrates the fact that br is indeed an almost constant parameter for this type of shots. Another important feature is that the Carbon lines previously measured in Carbon environment have dropped by a factor of 10 [16]. The br value of 11.36 measured on these series of shots is one of the largest that we have obtained in JET. It corresponds to a cocktail of impurities that have a high radiation yield per Zeff. As a consequence, even a moderate increase of Z_{eff} leads to a large fraction of the bulk energy being radiated away. For a reactor, this is of course unacceptable.

In Figure 5 are also plotted for comparison the data obtained in limiter mode. For both series of shots, only the data obtained in ICRH heating have been kept. The reason is that we found differences on the result of limiter plasmas when using different types of additional heating. The value of br that is found for limiter is 3.1. So in limiter, br is reduced by almost a factor of 4 compared to Divertor. The decrease of the br value in limiter case can be explained by the presence of light impurities in the bulk that are inefficient radiators in this region (increasing the denominator of relation 3). br can also be reduced if the high Z impurities are for some reason removed from the bulk in limiter operation. There is however no reason for this to happen as the ICRH additional heating is expected to create Tungsten erosion both in Divertor and Limiter operation. The difference in that case is therefore attributed to the behaviour of light impurities that are contaminating the bulk of the discharge in the case of Limiter and that are screened during Divertor operation.

We show next the effect of a change of confinement on the value of br. The data in Figure 6 are obtained in Diverted plasmas with ICRH only. These shots undergo H mode transitions back and forth. The energy stored in the discharges is not sufficient to trigger ELMS. These shots have

been studied and reported in conferences [17]. We have discriminated on the same plot the data corresponding to H and L mode phases. The result is that as far as these shots are concerned, discharges in L or H mode have almost the same br value (11.3) because the whole data can be fitted by only one linear function. This shows that the mixture of radiative contaminants in the bulk remains the same during the two phases. This result suggests that to change the value of br in an ILW discharge, a change of the impurity source is probably the most efficient mechanism, the transport properties of the discharge in the bulk not being seen here as the dominant controlling parameter for br.

6. EFFECT OF DIFFERENT TYPES OF ADDITIONAL HEATING ON THE VALUE OF βr

Figure 7, shows the result of a test of the scaling applied to discharges in L mode where 3 different types of additional heating have been used at low level (around 2 MW). When the plasma is diverted, all data are aligned regardless of the type of additional heating used. br is measured to be 11.9 and does not depend on the type of additional heating used. The value of br is consistent with the presence of high Z impurities in the bulk and with the screening of low Z impurities by the Divertor. In the same Figure are also plotted the results obtained in limiter plasmas. Here only a comparison between ICRH and Neutral beam injection (NBI) can be done because the Lower Hybrid heating is applied on diverted plasmas. Figure 7 shows that the result in this case depends on the type of additional heating used. The br determined with ICRH operation is 3.1 while the result obtained with NBI is only 1.3. The plasmas with NBI are much less radiative relative to Z_{eff} than the ones with ICRH. There are several ways to interpret this result. The contamination of low Z impurities could be higher in the case of NBI, or there may be less erosion of Tungsten produced by the NBI heating, or a combination of both of those. Some information can be gained by studying the spatial distribution of the radiation (low Z impurities radiate at the edge while high Z ones radiate everywhere). However, the br parameter gives global information about the radiative efficiency of the bulk impurities but does not allow discriminating exactly what species are radiating in the bulk. In order to determine this, a complementary spectroscopic analysis is always necessary.

7. DETERMINATION OF BR IN JET WITH CARBON ENVIRONMENT

We show here that the scaling derived in relation 1 fits also the bulk of discharges in Carbon environment. Figure 8 shows the result obtained on a series of 16 shots dedicated to a N2 seeding experiment. Some of the shots are performed without seeding and are intended as reference shots for comparison with seeded ones. All the others are performed with high levels of N2 injection. The parameters of these discharges are $I_p = 2.5MA$, $P_{NBI} = 13.3MW$, $P_{ICRH} = 1.5MW$ and the line density is above 2×10^{20} m^{-2}. During the additional heating phase of the discharge, for most of the shots, the ELMS undergo a change of frequency going from relatively frequent small ELMS to large type 1 ELMS. The ELMS are being filtered using the procedure described in section 4. The fit

is applied during the whole time window covering the occurrence of the ELMS. The βr parameter determined from the fit in Figure 8 is $\beta r = 0.89$. This has to be compared with the br value obtained with ILW in Divertor (11.3). This result shows that the impurities contaminating the bulk in Carbon environment are mostly very poor radiators per Z_{eff} compared to the ones contaminating the plasma in the ILW case.

This points towards contamination of the bulk by light impurities probably dominated by Carbon, the material of the Divertor, eroded both chemically and physically and also in this case, the absence of significant amount of high Z impurities. The value of br obtained in the carbon environment is reproducible and does not depend much on the details of the discharges provided that the plasma is diverted. All the plasmas that we have analysed yield values that differ by 50% at most from the value obtained in Figure 8. The result of Figure 8 is that the addition of other light impurities to the discharge such as N2 does not change dramatically the value of br in the Carbon environment. We display in the same Figure the fit of the bulk data in the case with and without N2 seeding. The two sets of data are almost superposed so that a unique fit can fit all the data. However, The fit of each set of data yields $\beta r = 0.55$ without N2 seeding and $\beta r = 0.83$ with N2 seeding. It is therefore probable that the addition of N ions to the bulk of the discharge produces a 50% increase of the br parameter with the Carbon environment. Finally we conclude that the average br value measured in the Carbon environment is bounded between 0.5 and 1. Compared with the one in ILW, it is decreased by at least a factor of 10.

8. THE INFLUENCE OF THE DIVERTOR RADIATION ON THE SCALING: COMPARISON WITH THE MULTI-MACHINE SCALING

The functional dependence of Zeff with the bulk radiated power and the density is the same than the one that is found by the multi machine scaling. Therefore, the two scalings must be related in some way. In order to study this, we are going to compare both of them by assuming that they are simultaneously verified. We write the multi-machine scaling as: $Z_{eff} = 1 + \alpha_m Prad/Ne^2$, where aM is the coefficient of the multi-machine scaling [8] and Prad the total radiated power. Usually, this scaling includes a dependence with the plasma envelope surface that is included in the aM parameter here. By combining the two scalings we get the relationship between the aM parameter (multi machine) and the ac parameter (bulk scaling). $\alpha_m = \alpha_c/(1 + Prad_{div}/Prad_{bulk})$. Equivalently we can write $\beta rm = \beta rc(1 + Prad_{div}/Prad_{bulk})$ (3). The inclusion of the Divertor radiation in the scaling is increasing the multi-machine brm value above the one measured in the bulk. We introduce the ratio $r = Prad_{div}/Prad_{bulk}$. For Carbon environment, brc is low (very little radiation in the bulk) and the main Carbon impurity is radiating in the Divertor so that r takes large values above 1. As a result, in Carbon environment brm is expected to be about r times above the bulk one. For Tungsten environment, brc is high and there is very little radiation in the Divertor, r is below 1 and brm is expected to be close to the brc value of the bulk. In order to verify this, we are going to analyse a shot in ILW in Ohmic where the density was increased and triggered a detachment in the Divertor.

Figure 9 shows the scenario of the shot. We are going to study three time windows of this shot. The first one between 45 and 50s is the limiter phase. The second one between 50 and 59s is in Divertor with X point with moderate variation of the mean density. In the last one from 59 to 63s, the density is increased and triggers a detachment in the Divertor.

We plot the scaling obtained for the limiter phase in Figure 10. In this case, the multi-machine scaling is exactly equivalent to the bulk one as all the radiation comes from the bulk. The brc or brm value deduced from the fit of the data is 1.42. This value is small and compatible with the presence of a high fraction of low Z impurities in the bulk.

The result of the second time window in Divertor is more difficult to interpret. We observe in Figure 11 that the term $Prad_{div}/Ne^2$ takes a limited range of values compared to the variation of Pradbulk/Ne2. The consequence is that $Prad_{div}/Ne^2$ can be considered almost as a constant C1. The multi machine scaling can therefore be written as: $Z_{eff} = 1 + \alpha_m C1 + \alpha_m Prad_{bulk}/Ne^2$. This expression shows that the multi machine scaling gives a brm value that should be the bulk brc value but the constant in the scaling is no more 1 but is increased by am C1. For this time window, brc is found to be 6.66 while brm is found to be 8.55. The two values are close as expected. This rather high value indicates that there are most probably some high Z impurities radiating in the bulk in spite of the fact that the discharge is in Ohmic. The prediction for Z_{eff} of the multi machine law departs from the Z_{eff} calculated from Bremsstrahlung in this case.

The third time window corresponds to the detachment phase of the plasma and for this time window, the plasma parameters change over a large range. Figure 13 shows that at these high densities (for an Ohmic shot), Zeff is almost a constant and its value is close to 1. The brc and brm of the discharge have to be determined in a different way. If we write $Prad_{bulk} = brc\ Ne^2\ (Z_{eff} - 1)$ for the bulk scaling, $(Z_{eff} - 1) = constant = C2$ gives $Prad_{bulk} = brc\ C2\ Ne^2$. As a result Pradbulk is a linear function of Ne^2 and the slope of linear fit allows to measure brc C2 and to recover brc. This is possible provided that C2 can be measured with some accuracy. In this case, the uncertainty on the average value of $Z_{eff} - 1$ is large as we find $C2 = 0.02$ with a standard deviation of 0.014. This will only allow to get a range of values in which brc must lie.

We plot in Figure 14 Prad as a function of Ne^2 for bulk, Divertor and total radiation. It is immediately clear on these curves that the linearity is only obtained for the bulk radiation. $Prad_{div}$ is not a linear function of Ne^2 as it tends to saturate for high values of Ne. The slope measured on the bulk radiation is 0.223 which yields brc comprised between 6.54 and 11.15 if we take into account the uncertainty estimated from the standard deviation of $Z_{eff} - 1$. In any case the value of brc is large and compatible with what was found during the second time window before the density was raised. It is possible to estimate the value of brm during this detachment phase in the same manner. In Figure 14 we note that the addition of the Divertor radiation to the bulk radiation damages the linearity that is observed with bulk radiation only. However an average slope is obtained at 1.01 which gives βrm between 27.9 and 50.5 We note that some qualitative coherence with relation 3 is observed as $\beta rm > \beta rc$.

The result that is obtained here is that the relatively limited radiated power observed in the core is the result of the extreme dilution of the impurities as the brc parameter remains large (and is probably unchanged compared to the second time window). As far as brm is concerned, it is extremely large and becomes compatible with relation 3. However it has no clear physical meaning, as firstly the Z_{eff} in the Divertor is probably not the one in the bulk and secondly the radiation in the Divertor during detachment can include radiative recombination of the deuterium that is not related at all even to a change of a local value of Z_{eff}. However, the prediction of Z_{eff} by the multi-machine scaling is not far from the measurement i.e., it is close to 1. The results obtained here show that the multi-machine scaling in ILW describes mostly the bulk behaviour except at the detachment where its prediction of Z_{eff} is close to the measurements. We note also that at very high densities where Z_{eff} tends towards 1, the determination of brc can become difficult. In that case lower densities phases of the same plasma can be used because the brc parameter is a very robust parameter (i.e. the distribution of impurities radiating in the bulk does not change that much).

9. COMPARING THE RADIATIVE EFFICIENCY OF DIFFERENT DISCHARGES USING THE BR PARAMETER.

According to relation 3 in section 4, $\beta r/V$ characterizes the radiative properties of the impurities in the bulk of a machine regardless of their amount. There is in this parameter no information about the radiative performance of the discharge itself. A discharge can have a very high value of βr with very little bulk radiated power if the Z_{eff} is maintained sufficiently low. In order to compare the radiative efficiency of the bulk of discharges that can be very different, we are going to define an "equivalent" discharge. An equivalent discharge, is an ideal discharge that has the same Z_{eff}, $Prad_{bulk}$ and Ne than the real discharge, it has also the same volume V. It is composed of only one type of ion that has an individual charge Z_{eff}, the number of these ions being $N_{eq} = Ne/Z_{eff}$. We suppose also that this ideal discharge radiates uniformly over its volume. It radiates macroscopically as the real discharge in the sense that it obeys the same scaling law than the real one with the same βr value.

We can write the radiated power of this ideal discharge as:

$$Prad_{bulk} = Ne^2 \, Lz \, V/Z_{eff}$$

where Lz is the radiative function of the “equivalent” discharge. This Lz function can be calculated for any discharge but it is related to br in the following way. Because the "equivalent discharge obeys the same scaling law than the real one,

$$Prad_{bulk} = Ne^2 \, (Z_{eff} - 1) \, \beta r,$$

the radiative function Lz of the equivalent discharge can be written as a function of βr as:

$$Lz = Z_{eff}(Z_{eff} - 1) \, \beta r/V$$

As this function Lz is defined in a unique way for any type of discharge, it can be used to compare

different discharges and even the radiative performance of plasmas in different machines. Lz is only a function of Z_{eff} and of the normalised parameter βr/V that contains all the atomic physics of the impurities radiation in the real discharge.

Lz does not describe the radiative function of the real discharge but it is related to this function in the following way. If we assume that the impurity radiation of the real discharge can be written as in section 4 like:

$$\Pr ad_{bulk} = NeV \sum_k N_{imp}^k \sum_i a_i^k b_i^k c_i^k Lt_i^k$$

We get $Lz = \frac{\sum_k N_{imp}^k \sum_i a_i^k b_i^k c_i^k Lt_i^k}{N_{eq}}$. As N_{eq} is a fraction but has the same order of magnitude as Ne and as the total amount of impurities is in general very small compared to N_{eq}, the Lz of the "equivalent" discharge will be smaller than the one of the real discharge by several orders of magnitude (typically 3 in ILW). The radiative function Lz of the "equivalent" discharge must be minimized to reduce the radiative performance of the bulk of the real discharge. By construction this function Lz does not give any information about the spatial structure of the radiation as it assumes that the radiation of the "equivalent" discharge is homogenous over its volume.

Two discharges with very different impurity ions can have about the same Lz, but the discharge with the low Z impurity will radiate only at the edge, while the one with the high Z impurity will radiate everywhere in the bulk. In fact, a rough information about the localisation of the radiation is given by the value of br, as was discussed above.

We propose to compare the radiative efficiency of the bulk plasma for two discharges of JET at high power, one in the Carbon environment and another one in ILW. The one in carbon corresponds to a reference shot used for comparison with discharges with N2 seeding. The total applied power is 15MW with 13MW of NBI power, the remnant being shared between ICRH and Ohmic power. The second discharge was obtained at the end of the 2012 campaign in ILW. This discharge was heated with 22MW of total power with 17.2MW of NBI power and 4 MW of ICRH power. In order to pace the ELMS, that are known to be a strong source of Tungsten, vertical "kicks" were applied to the plasma at 20kHz. First the br of the two discharges can be calculated by using the fit of expression 1. The usual plot is shown in Figure 15. For the shot in Carbon environment $\beta r = 0.89$ is found, in the usual range of values encountered for this type of environment. For the ILW, $\beta r = 10.7$ is found, a value compatible with the presence of high Z impurities in the bulk of the discharge.

The Lz of the equivalent discharges for these two shots is plotted in Figure 16. During the NBI phase, Lz goes from 1 to 3×10^{-34} Wm^3 for the carbon environment shot while it varies between 4 and 4.5×10^{-34} Wm^3 for the ILW shot. The reduction of the Lz in the ILW shot is obtained with the reduction of Z_{eff} (less erosion by pacing of the ELMS with the periodic vertical kicks). We note also that Lz dramatically increases at the end of the discharge, from 7s on. This comes from the cessation of the vertical kicks and the reduction of the additional heating power and density. In the Carbon environment, the low value of Lz comes from the initial low br value, indicating the absence

of significant amounts of high Z impurities in the bulk. Figure 16 highlights the relative success of the procedure that was followed during shot 83398 with the vertical kicks. As a result the radiative efficiency of the "equivalent" discharge is only 2 times the one obtained in Carbon environment.

10. CONSEQUENCE OF HIGH βr : OPERATIONAL REGIME OF JET IN ILW WITH HIGH Z IMPURITIES IN THE BULK

The high br value (11) that is very often encountered in the ILW configuration has consequences on the operational domain in JET. The radiation in the bulk can become the limiting factor for the stability of the discharge and in order to decrease it, it is necessary to operate the discharge at very low Z_{eff}. This is what is being done in the case of Figure 16 with shot 83398. However, it is possible to define more accurately the maximum value of Z_{eff} for which the radiation equates the total power and also the maximum Z_{eff} value necessary to obtain a predefined radiated fraction. If we write $Prad_{bulk} = r_f$ Ptot, where Ptot is the maximum power applied to the discharge in MW. Relation 2 gives:

$$r_f = Ne^2 (Z_{eff} - 1) \beta r / Ptot \qquad (4)$$

This allows to calculate the radiated fraction for any type of discharge as a function of Z_{eff}, provided Ne, br and Ptot are known. We present in Figure 17, the result that is obtained for the case of Figure 16, $Ne = 1.6 \times 10^{20}$ m^{-2}, $P_{tot} = 22$MW. We plot also the experimental data for comparison. The maximum Z_{eff} corresponding to $r_f = 1$ is found to be around 1.85 for the specified parameters. This shows that the operational domain is very constrained by the value of Z_{eff}. During most of the phase where the vertical kicks are applied, Zeff is around 1.3 but an
increase of 0.5 with the same br would lead to a radiative collapse. As the parameters of the discharge are evolving in time, the maximum Z_{eff} corresponding to $r_f = 1$ can also be plotted as a function of time. Figure 18 shows that after 55s, the additional heating level is decreased and the maximum Z_{eff} is reached transiently putting the discharge at risk.

However, further on, Ne is rapidly decreased allowing the discharge to end quietly. These results indicate that it is always possible to calculate the operational domain of a machine relative to the core radiation once the br of the plasma has been measured.

11. ONE STEP FURTHER: BR CONSIDERED AS A DYNAMICAL PARAMETER

The parameter βr has been determined as a time average value calculated over sufficiently large time windows during one shot or a series of shots. It has been found to be robust through main plasma parametric changes such as density, level of additional heating etc. However it is questionable if the relation written in 1 is only verified in a statistical way or if the dependence that links $Prad_{bulk}$, density and Z_{eff} is more profound and holds at all times. This idea is natural as βr describes the distribution

of the radiation among various ionisation levels of various impurities. There is no reason why this distribution should remain completely constant throughout time. In that case the "dispersion" that is observed around the linear fit of relation 1 is not random but structured and its meaning may be that br takes different values at different times. In order to test this idea we re-analyse the shot 83398 already discussed in section 11. We first observe in Figure 15 that the dispersion is clearly not random as the data seems to be grouped in packs at $Prad_{bulk}/Ne^2$ around 2 and $6.5MW/10^{40}$ m^{-4} and even seem to define different slopes at these values. This could be simply the result of a βr value different from the average one. In order to test this, we plot in Figure 19 $\beta r(t) = Prad_{bulk}(t)/(Ne^2(t)\ (Z_{eff}(t) - 1))$. We observe that during the vertical kicks applied to the plasma βr is about constant and takes a value of about 6.8. This is 37% less than the value determined from the slope of Figure 15. We observe also that at the end of the kicks after 55s, βr jumps to 10, the standard value that is obtained in most of the shots in ILW. So it seems that the slope inferred from figure 15 is the one that is related to what is occurring after 55s. This is consistent as the largest changes of $Prad_{bulk}/Ne^2$ occur after 55s. As a result, the plot of Figure 15 is misleading as it yields a value of the slope that does not correspond to the time window of the vertical kicks. In fact, Figure 19 shows that the vertical kicks are efficient both in reducing the Z_{eff} and the br of the discharge. The consequence of this lower value of br is that the operational domain constrained by the value of Z_{eff} during the kicks and defined in section 12 is too pessimistic. With this new value of βr, Z_{eff} values up to 2.1 can be reached before the radiated fraction gets to 1.

As we consider now br as a variable parameter that is no more measured statistically, it is possible to evaluate its uncertainty. A simple calculation of uncertainties gives

$$\frac{\Delta\beta_r}{\beta_r} = \frac{\Delta \Pr ad_{bulk}}{\Pr ad_{bulk}} + 2\,\frac{\Delta Ne}{Ne} + \frac{\Delta (Z_{eff} - 1)}{Z_{eff} - 1}$$

The total relative uncertainty is very sensitive to the relative uncertainty on Ne. If we take $\frac{\Delta (Z_{eff} - 1)}{Z_{eff} - 1}$ and the other relative uncertainties to be about 10%, we get a total relative uncertainty of about 40%.

The result plotted in Figure 19 shows that time variations of br are really correlated with parametric changes in the discharge and tends to confirm that the br calculated at all times (ELMS filtered) has indeed a physical meaning. As a result, situations where no average slope can be found to fit expression 1 can be studied. This is seldom observed but there are some shots with N2 seeding where this situation is encountered. This simply means that br "the radiative efficiency of the impurities mixture» is changing continuously as a function of time. It is the result of the continuous leakage of Nitrogen to the bulk of the discharge.

Another case, where such a situation is encountered is the case when an increase of the radiation as a function of time takes place although the main parameters of the plasma are kept constant. This situation was observed during the first campaign of JET in ILW during experiments to get the base line H mode scenario. We are going to compare the behaviour of two shots, One at the very

beginning of the ILW campaigns, where ICRH was the main heating system that displayed a high radiation fraction but where the radiated power remained constant throughout the additional heating phase (shot 80760). The other one is a shot that was performed later and aimed to get an H mode with NBI heating (shot 81913).

The scenario of this shot is plotted in Figure 20, it is a shot heated up with 8 MW of NBI heating. It belongs to the experiments that were performed to obtain the baseline H mode scenario at 2 MA. The other one (shot 80760) is operated with 3 MW of ICRH additional heating in L mode (Figure 21). Both shots have a high radiated fraction but in shot 81913 the radiated power is increasing strongly during the NBI heating phase.

Although it is possible to determine an average value for br for both shots, it is doubtful that this will give account of the increase of Prad during NBI heating in shot 81913. Therefore br is calculated as a function of time as above. It is plotted in Figure 22 for the two discharges. The br obtained in the case of ICRH heating is very high with a value around 15 during most of the additional heating phase. This result is consistent with the one of other ICRH discharges where an average value of br was obtained by calculating an average slope between Z_{eff} and $Prad_{bulk}/Ne^2$. The value of br obtained for the NBI heating case increases from 5 to 9 during the 3s of the additional heating phase. However, It remains from 2 to 3 times lower than the one obtained with ICRH heating in shot 80760. This confirms that in the case of NBI heating the "cocktail" of impurities polluting the bulk has a much less radiative yield per Zeff than in the case of ICRH heating. Comparing the LZ of the two discharges shows that the ICRH one is much more radiative. The Lz of the ICRH discharge is around 6 and is at least three times higher than the one of the NBI discharge that goes from 1 to 2. Relatively to the ICRH heated discharge, the NBI heated one does not have a very high radiative efficiency even at the end of the Prad increase.

A second observation is that the Z_{eff} of this discharge remains about the same although the density is increased. This indicates that the amount of impurities does increase as Z_{eff} should decrease with Ne with no additional impurity contribution. The data reveals that the reason for the radiated power increase during NBI comes from two mechanisms that are adding together. The first one is the increase of the line density that goes from 1.2 to 1.9×10^{20} m^{-2} during the NBI heating phase. This term is very efficient as through relation 2, $Prad_{bulk}$ scales with Ne^2. If this was the only term changing during the $Prad_{bulk}$ increase, $Prad_{bulk}$ would be a linear function of Ne^2. This is not the case. Although $Prad_{bulk}$ does increase with Ne^2, the increase is stronger than linear, indicating that something else is at work. The second cause is the increase of βr from 5 t o 9. This increase indicates a change in the distribution of radiation among the impurities with a larger contribution of the ones that have a higher Lt/zi^2 (according to relation 3). This is compatible with an increase of the Tungsten or any high Z material concentration in the bulk.

In fact the events taking place during this shot are complicated and changes in the spatial distribution of the radiation and the temperature profile are observed. We show in figure 24 the changes monitored on the bolometry vertical and horizontal profiles during the increase of Pradbulk.

Figure 24a shows the line integrated signal on the horizontal lines of sight that are scanning the plasma in the vertical direction. The first 2 channels at the bottom of the machine monitor the radiation in the Divertor and X point region. The last channels correspond to the top of the machine. Figure 24 left shows that the radiated power increases only in the central region of the plasma around the mid-plane. The increase is seen at all times during the additional heating but really explodes between 51 and 52s. On the horizontal profile (figure 24, right) that goes from high field side to low field side, a peak of power is seen at all times in the centre and remains constant throughout time. It corresponds to the radiated power in the Divertor. More interestingly, the radiated power is seen to increase on the low field side while remaining unchanged everywhere else. This increase corresponds to the central increase observed on the vertical profile. Therefore the increase of the total radiated power takes place around the mid-plane on the low field side. Another observation is the decrease of the electron temperature on the low field side during the additional heating phase, the profile becoming hollow around 51.8s. It is possible to discuss at least qualitatively what effects must be associated to the change of βr. We have seen in the paper that the value of βr in ILW is very robust and that about the same value (around 11) can describe a large number of diverted shots covering different parametric changes. The same value is recovered in L or H mode with different levels of additional heating and therefore different central Te values and different Te profiles. This shows that βr is very resilient to the changes of the temperature profile. As a result it is doubtful that the change in the temperature profile can give account for the almost doubling of the br value throughout the additional heating phase. These comments indicate that the increase of the radiated power in this particular region is also associated to an increase of the concentration ε_k of high z impurities, the main suspect being Tungsten.

Finally, it now seems that relation 4 that predicts the radiated fraction to depend linearly on Z_{eff} is too optimistic for this particular case. This relation does not take into account the changes of βr that are monitored in shot 81913 so that the maximum Z_{eff} to get the radiated fraction to 1 is decreased relative to relation 4.

12. βr MEASURED IN AN OTHER MACHINE: TORE SUPRA

In this section we report the $\beta r/V$ obtained in standard conditions in Tore Supra (TS) [18] that is a Carbon based Limiter machine running in L mode. Its volume is about 24 m^3 with a small radius of $a = 0.72$ m, $R = 2.38$ m. Apart from the Ohmic heating, it is heated exclusively with ICRH and LH waves. It is equipped with a pumped Toroidal limiter made up of Carbon that is physically eroded during the discharge. As a result Carbon is the dominant impurity and gives account for most of the radiation [19] that is concentrated above the limiter. We will compare the $\beta r/V$ of this machine with the one obtained in JET in Carbon environment in Ohmic mode Limiter.

The scenario of the shot in TS is presented in Figure 25. The shot starts with 4 seconds of Ohmic plasma from 2 to 6s. The second time window extends from 6 to 15s during which about 4.5 MW of ICRF waves are applied to the plasma. At 15s, the ICRF heating power is decreased to 1MW and

about 1.9MW of LH power from 2 antennas is applied to the plasma. These events define 3 time windows that give specific results for the value of βr/V visible in Figure 26. The first and third time windows give a βr/V of about 0.34. This value is the standard value that is observed in Tore supra for ohmic and low power shots. During the ICRF phase, βr/V is decreased to 0.28. Although br/V displays some variations, they remain limited and βr/V remains at a value close to 0.3. As a result a unique scaling that gives reasonable results can be applied for the 3 time windows.

As far as the JET data is concerned, we have selected shots from disruption experiments performed in one of the 2008 campaigns. During these shots in Ohmic, the density was raised at the end of the discharge triggering a disruption. For the first five seconds of the plasma current plateau, the discharge is run in limiter mode, and then the X point is formed. During the limiter phase, the radiated power is located on the high field side in the mid-plane in a MARFE state. After formation of the X point, most of the radiation comes from the Divertor region. The scenario of the shot is displayed in Figure 27 while the time dependent br is plotted in figure 28. Two things have to be noted about the result of Figure 28. First of all, although, the radiated power spatial distribution and level in the bulk is completely different between the limiter and Divertor phases, both time windows yield very close br values. Secondly, the value of βr/V that is obtained (0.015) is more than ten times smaller than the one obtained in Tore Supra.

According to these results, in Carbon environment, the impurities in TS are much more radiative per Z_{eff} than in JET.

One of the explanations for this difference may be that the volume occupied by the radiative ions in case of light impurities does not increase linearly with the volume of the machine. In case of light impurities, the radiative layer is confined at the edge of the plasma where the temperature is cool enough for the ions to radiate. The width of the radiating layer is expected to be controlled by the temperature profile but the most important process that is believed to determine its size is the anomalous turbulent transport. If we suppose that in case of light impurities the width of the radiative layer of the ion of charge i is Di, we can express the dependence of the ratio ri of the volume occupied by this ion as a function of the plasma dimensions: $ri \approx S\ D_i/V$ where S is the envelope of the plasma and V its volume. In the simplest case corresponding to the cylindrical case, $S = 4\ \pi^2\ a\ R$ and $V = 2\ \pi^2\ a^2\ R$ with a and R respectively small and large radius, gives $ri \approx 2D_i/a$. If Di does not increase in proportion with the small radius a, ri will get smaller for larger a values. As a result the parameter c_i^k in relation 3 will decrease when the small radius of the plasma, a, increases. The consequence of this is that br /V is expected to be smaller in large machines. Of course, these considerations do not apply to high Z impurities that can radiate everywhere in the plasma volume.

CONCLUSION

The main result of this paper is that during quiet phases of the plasma, Pradbulk is a function of Zeff, Ne and a parameter br that describes the radiative efficiency of the impurity mixture. Furthermore, the relation between these parameters is found to hold at all times during parametric plasma changes

provided that these changes are not too violent (ELMS must be filtered). The relation is also independent from the state of the plasma that can be in H, L or Ohmic mode, limited or diverted. An average br parameter can be determined by fitting a discharge or a series of discharges with relation 1. βr describes how much power is radiated in the bulk relative to Z_{eff} and the density. One of the main results is that br is found to vary little for Divertor operation from shot to shot for a given wall and Divertor configuration. Its value is also quite insensitive to the radiated power spatial distribution. In fact, it seems to depend mostly on the nature of the wall and Divertor materials. br is found to be about 11 in ILW plasmas while it is around 1 for JET Carbon environment plasmas. The robustness of the br value, considering the complexity of all the atomic physics, profile effects and transport which could perturb is a striking result.

The value taken by br gives indications about the type of impurities polluting the discharge. A large br value indicates contamination of the bulk by high Z impurities while a small br indicates absence of this type of impurities. Most importantly, βr is not a statistical parameter but has a meaning at all times. It can be calculated as a function of time during quiet phases and allow studying individual discharges. Its changes always indicate changes in the composition of the impurities mixture.

The high values of βr measured in JET ILW put some constraints on the operational domain of the discharges. It is limited by a maximum Z_{eff} value (or a maximum density if Z_{eff} cannot be controlled) that can be calculated and must not be reached if a disruption by radiative collapse has to be avoided. The high values of br measured in JET in ILW indicate that this parameter will probably also be high in ITER. As a result the problem of core radiation will very probably also be central for the operation of ITER.

ACKNOWLEDGMENTS

This work was supported by EURATOM and carried out within the framework of the European Fusion Development Agreement. The views and opinions expressed herein do not necessarily reflect those of the European Commission

REFERENCES

[1]. V. Rohde et al., Nuclear Fusion **49** (2009) 085031
[2]. T. Loarer, Journal of Nuclear Materials **390–391** (2009) 20–28
[3]. C.H. Wu, U. Mszanowski, Journal of Nuclear Materials **218** (1995))
[4]. A. Kallenbach et al 2009 Nuclear Fusion **49** 045007
[5]. R. Neu et al, Journal of Nuclear Materials **313–316** (2003) 116–126
[6]. J.C. Fuchs et al., 35th EPS Conference on Plasma Phys. Hersonissos, 9 - 13 June 2008 ECA Vol.32D, P-2.012 (2008)
[7]. G.F. Matthews, Physica Scripta **T145** (2011) 014001
[8]. G.F. Matthews et al., Journal of Nuclear Materials **241-243** (1997) 450
[9]. A. Loarte et al, Plasma Physics and Controlled Fusion **44** (2002) 1815–1844

[10]. P. Devynck, P. Ghendrih, and Y. Sarazin, Physics of Plasmas **12**, 050702 (2005)
[11]. H. Meister et al, Review of Scientific Instruments **75**, 4097 (2004)
[12]. R. Pasqualotto et al., Review of Scientific Instruments **75**, 3891 (2004)
[13]. A. Huber et al., Fusion Engineering and Design **82** (2007) 1327.
[14]. D.E. Post et al ., Contribution to Plasma Physics **36** (1996) 2/3, 240-244
[15]. M. Greenwald et al, Nuclear Fusion, Vol.**28**, No. 12 (1988)
[16]. S. Brezinsek, P1-083, "Residual Carbon Content in the Initial ILW Experiments at JET",20th International Conference on Plasma Surface Interactions in Controlled Fusion (Aachen, 2012)
[17]. C.F. Maggi et al., 39th EPS Conf. on Plasma Physics (Stockholm) 2012.
[18]. B. Beaumont, Fusion Engineering and Design Volumes 56–57, October 2001, Pages 667–672
[19]. P. Devynck et al., Nuclear Fusion **52** (2), 023007

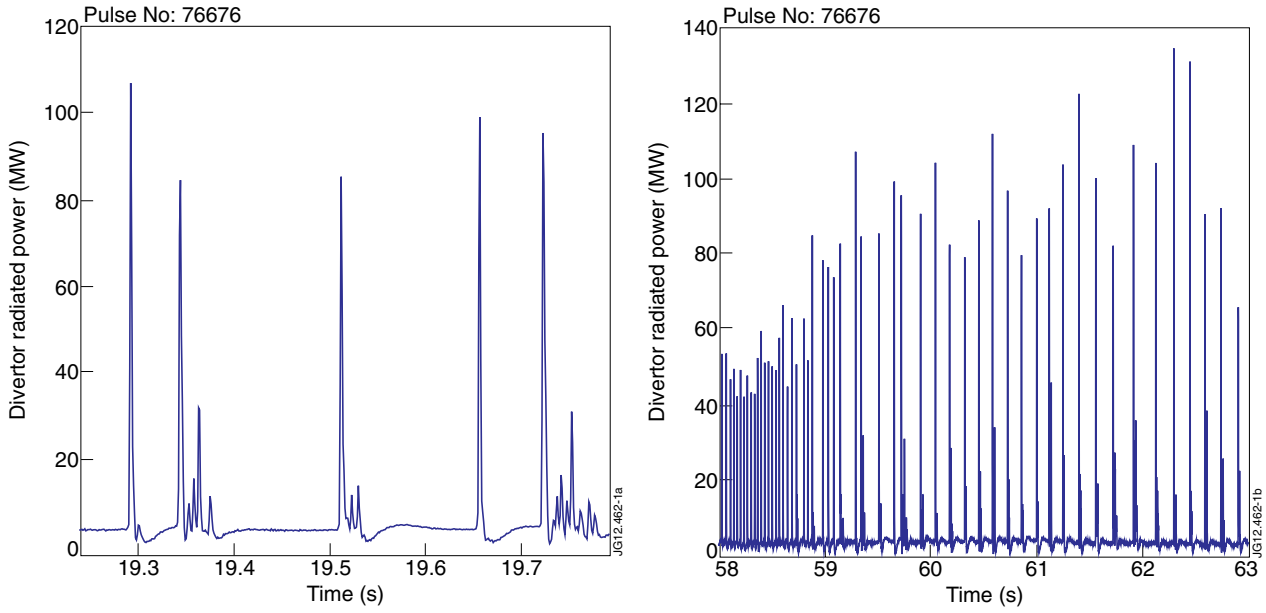

Figure 1: Left: thermography signal on tile 5 during NBI heating and N2 seeding. Right: details from same signal showing that the ELMS are grouped in packs of successive relaxations separated by larger waiting times.

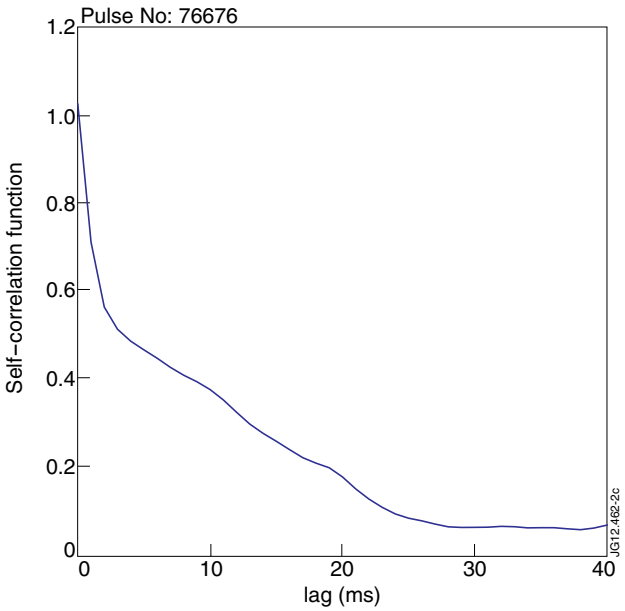

Figure 2: Self-correlation function of thermography signal on tile 5 during the time interval displayed in Figure 1.

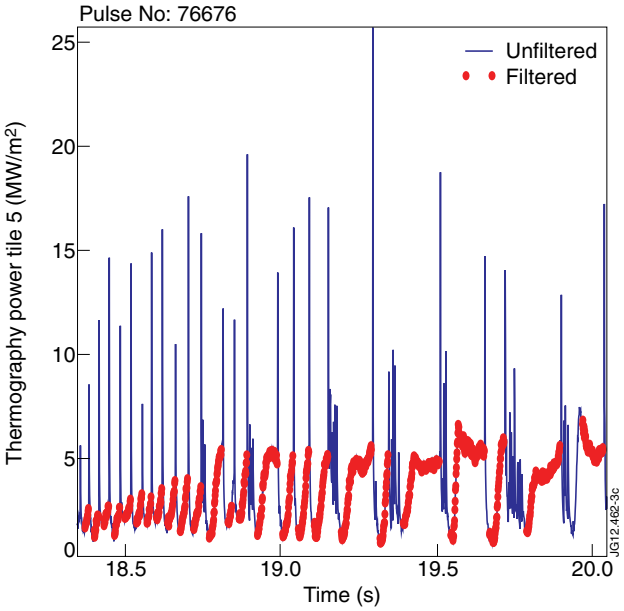

Figure 3: Result of the ELM filtering on the thermography signal of tile 5.

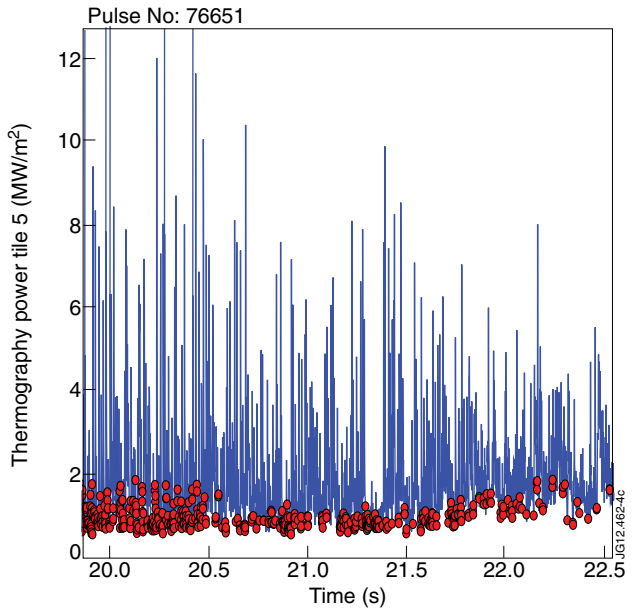

Figure 4: Result of the ELM filtering on thermography signal of tile 5. For this shot, the ELMS form a continuum of peaks and no frequency can be derived. Blue line: thermography signal.

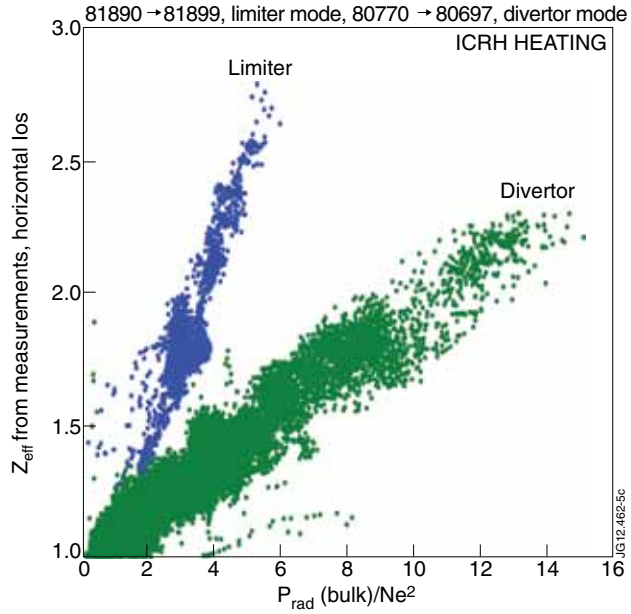

Figure 5: Z_{eff} as a function of $Prad_{bulk}/Ne^2$ for series of shots in Limiter and Diverted configuration ILW configuration. L mode with ICRH heating. Red dots: selected times by the filtering.

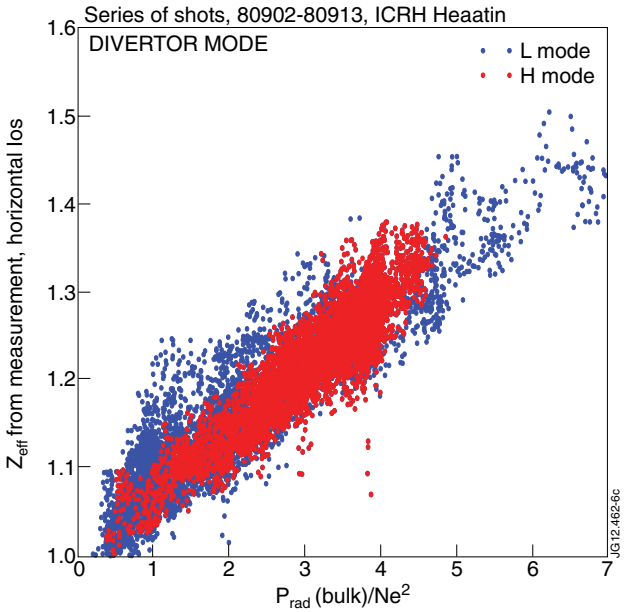

Figure 6: Z_{eff} as a function of $Prad_{bulk}/Ne^2$,ILW configuration. ICRH heating only. The shots underwent forward and backwards transitions from L to H mode: blue - L mode, red – H mode.

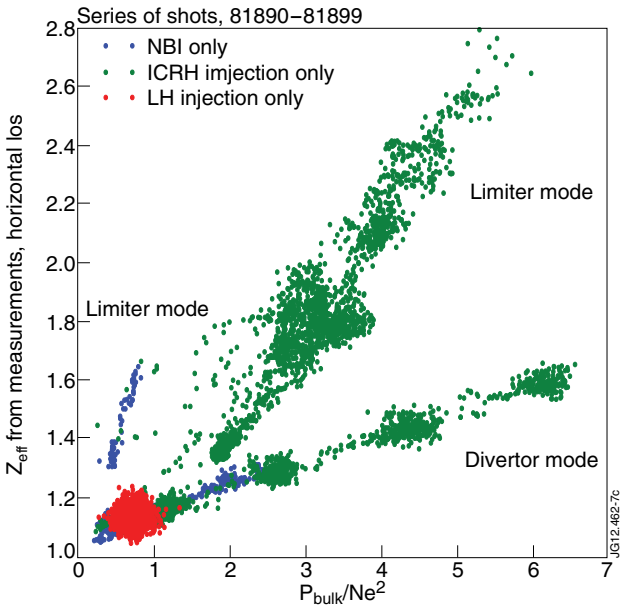

Figure 7: Comparison between Divertor and Limiter with several types of additional heating in ILW configuration, blue- NBI, green- ICRH, red - LH heating.

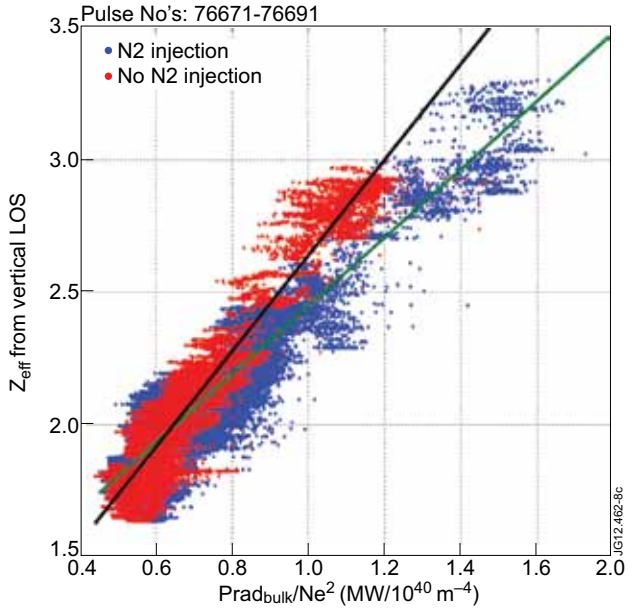

Figure 8: Z_{eff} as a function of $Prad_{bulk}/Ne^2$. Carbon environment, NBI additional heating. red with N2 seeding, blue without N2 seeding.

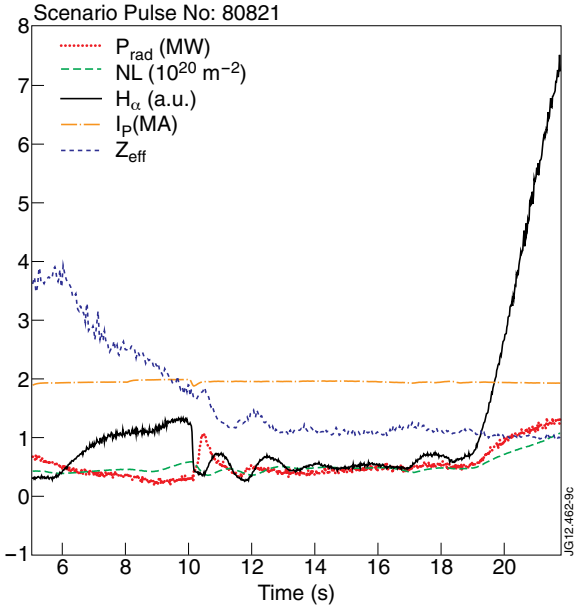

Figure 9: Scenario of an Ohmic shot in ILW where a detachment was triggered in the Divertor by increasing the Deuterium density.

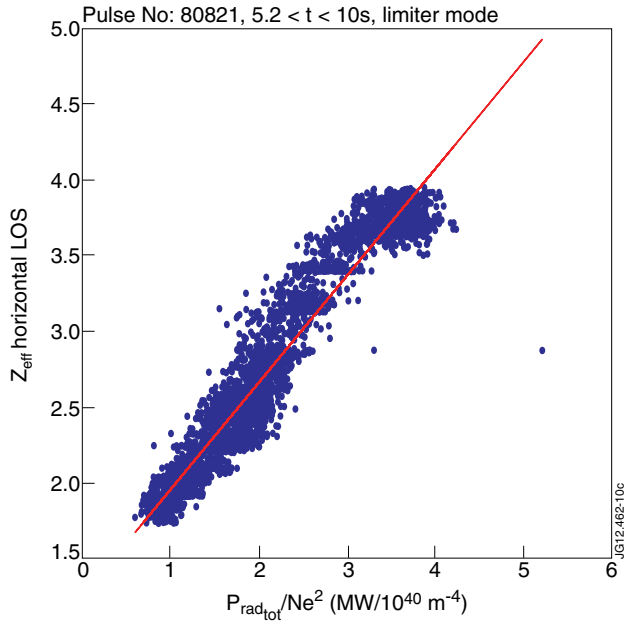

Figure 10: Test of the Multi-machine scaling equivalent to bulk scaling during limiter phase of Pulse No: 80821.

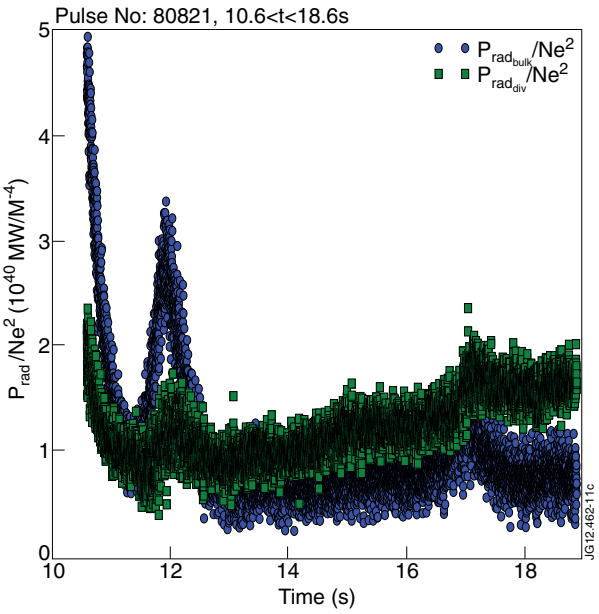

Figure 11: $Prad_{bulk}/Ne^2$ (blue) and $Prad_{div}/Ne^2$ (green) as a function of time during second time window of Pulse No: 80821, Divertor phase.

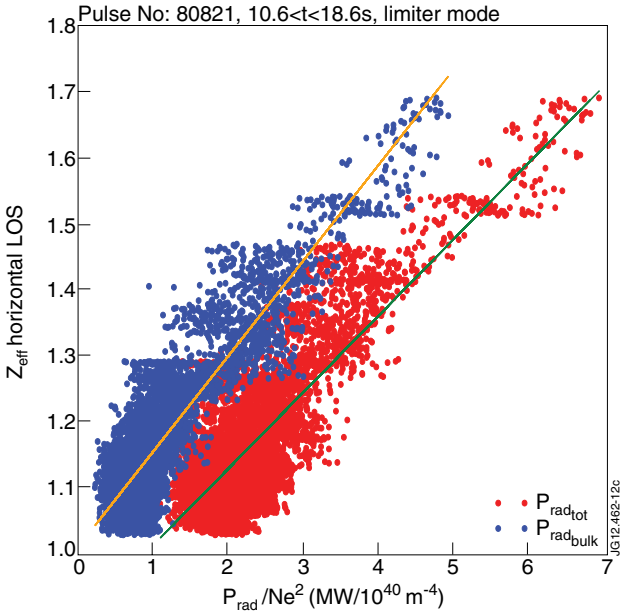

Figure 12: Comparison of bulk scaling (blue) with multi-machine scaling (red). second time window of Pulse No: 80821.

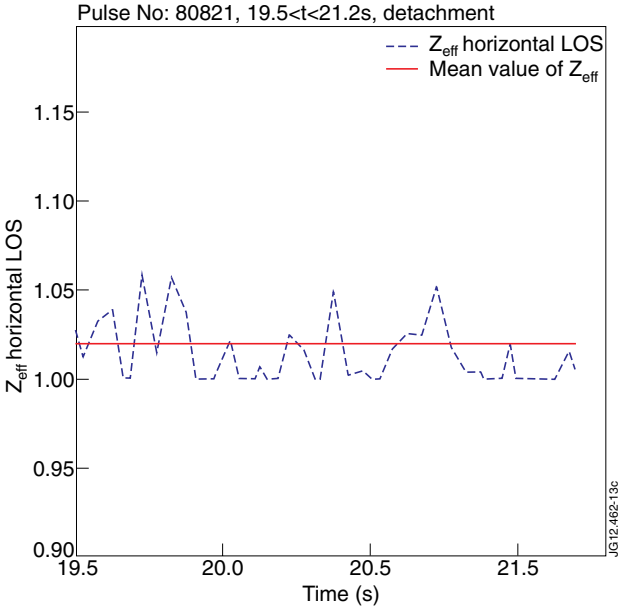

Figure 13: Value of Z_{eff} as a function of time during the detachment phase of Pulse No: 80821.

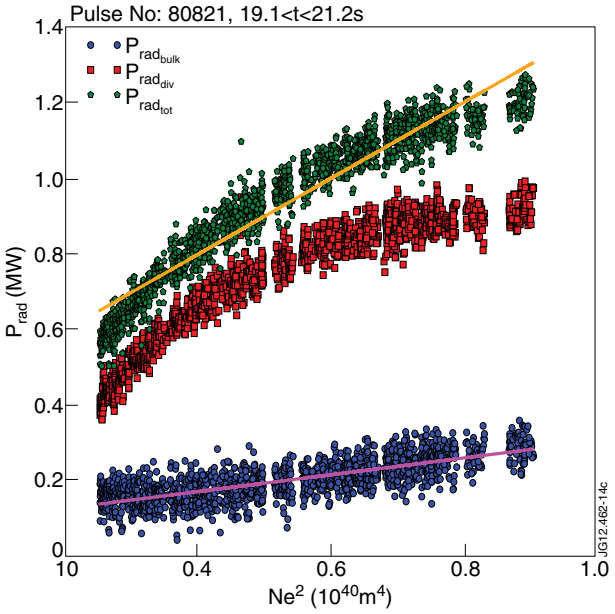

Figure 14: P_{rad} as a function of Ne^2 during detachment phase of Pulse No: 80821, blue bulk, red Divertor, green, total.

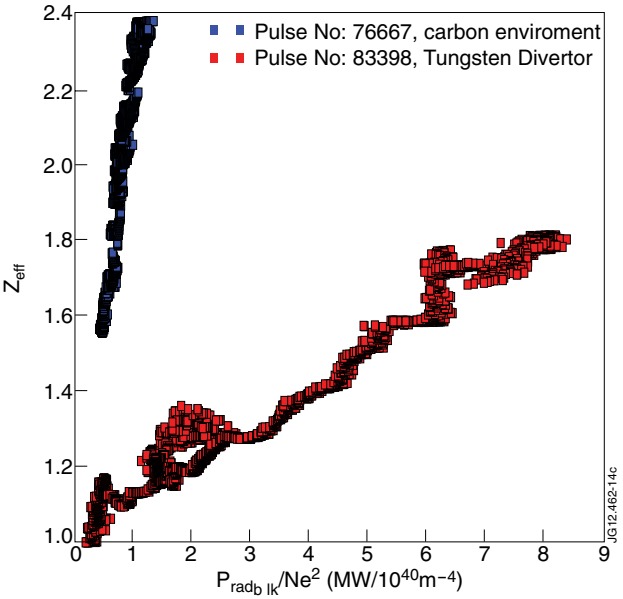

Figure 15: Z_{eff} as a function of Pradbulk/Ne^2 for two high power discharges. blue, Pulse No: 76667 Carbon environment, red, Pulse No: 83398 ILW.

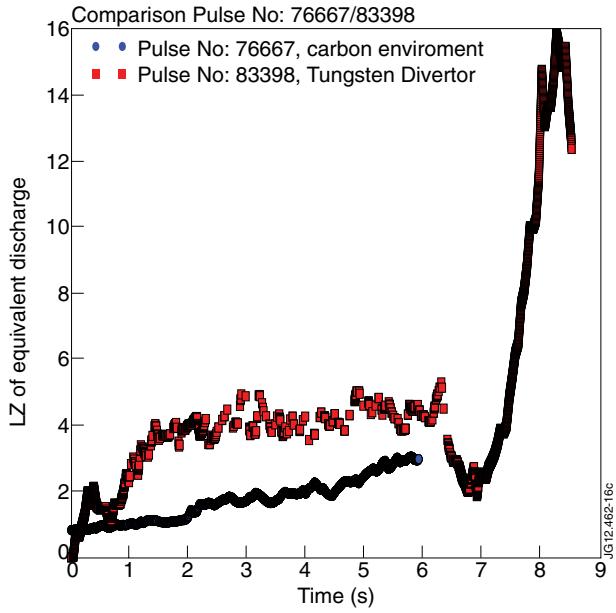

Figure 16: Lz as a function of time, calculated for the two discharges of Figure 15.

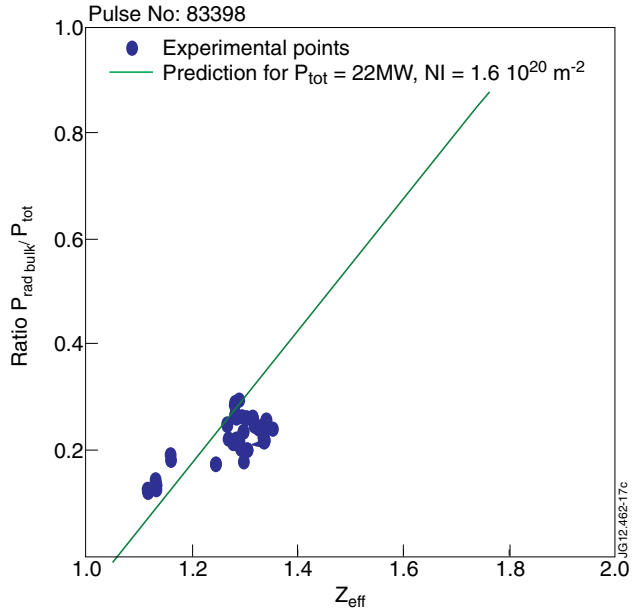

Figure 17: Ratio Pradbulk/Ptot as a function of Z_{eff} deduced from relation 4 for Pulse No: 83398.

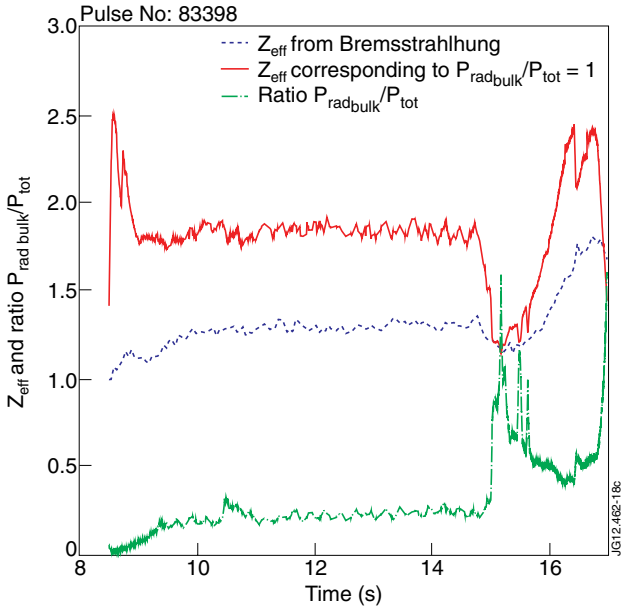

Figure 18: Plot of Z_{eff} from Bremsstrahlung (blue), Z_{eff} for rf=1, (red), and experimental ratio $Prad_{bulk}$/Ptot as a function of time during the vertical kicks, Pulse No: 83398.

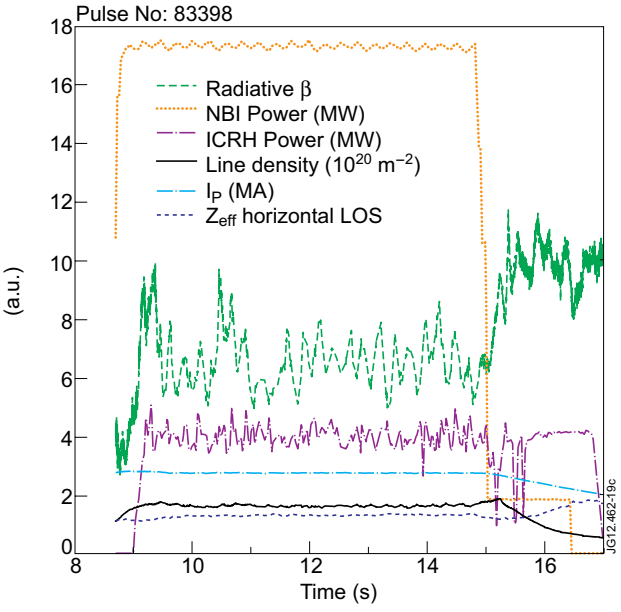

Figure 19: Pulse No: 83398, βr (blue) calculated as a function of time, assuming that relation 2 is not statistical but holds all the time.

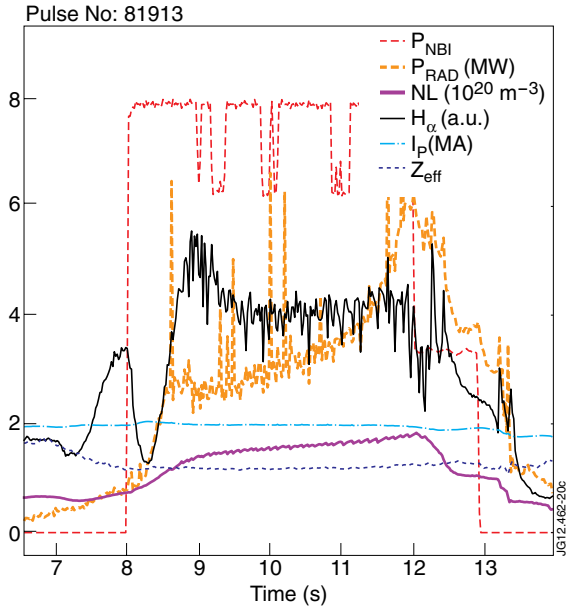

Figure 20: Scenario of Pulse No: 81913.

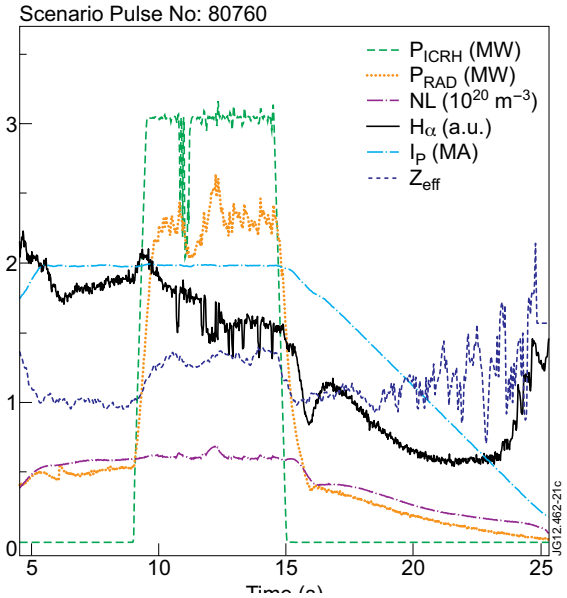

Figure 21: Scenario of Pulse No: 80760.

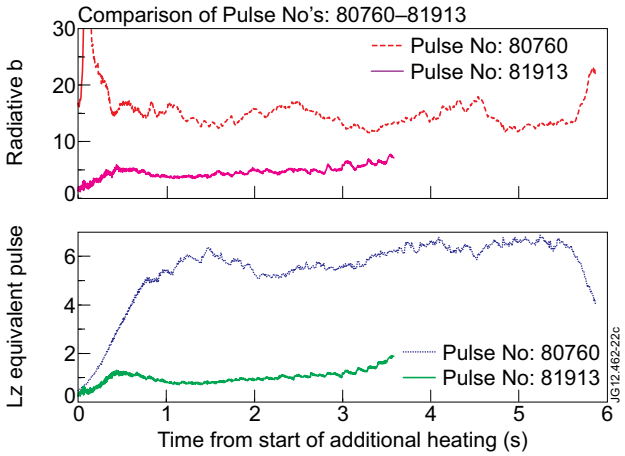

Figure 22: Comparison of βr and Lz during additional heating for Pulse No's: 80760 and 81913.

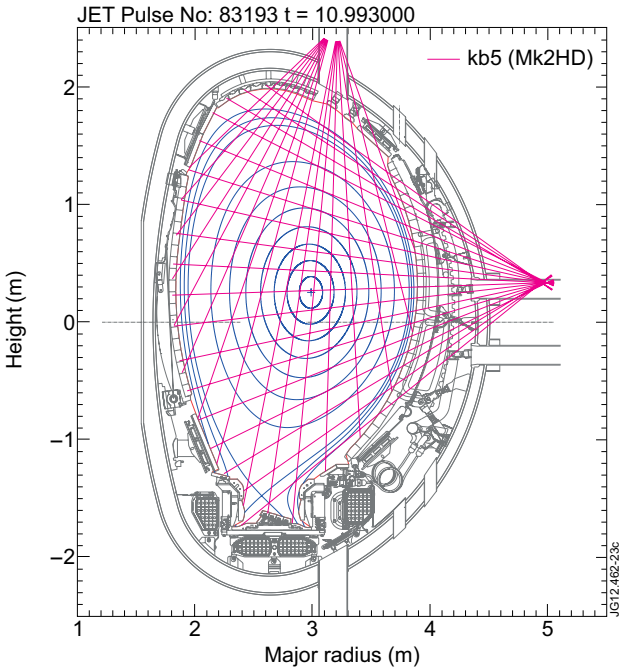

Figure 23: Line of sights of the KB5 bolometer used to visualize the vertical and horizontal profiles of the radiated power in Figure 24.

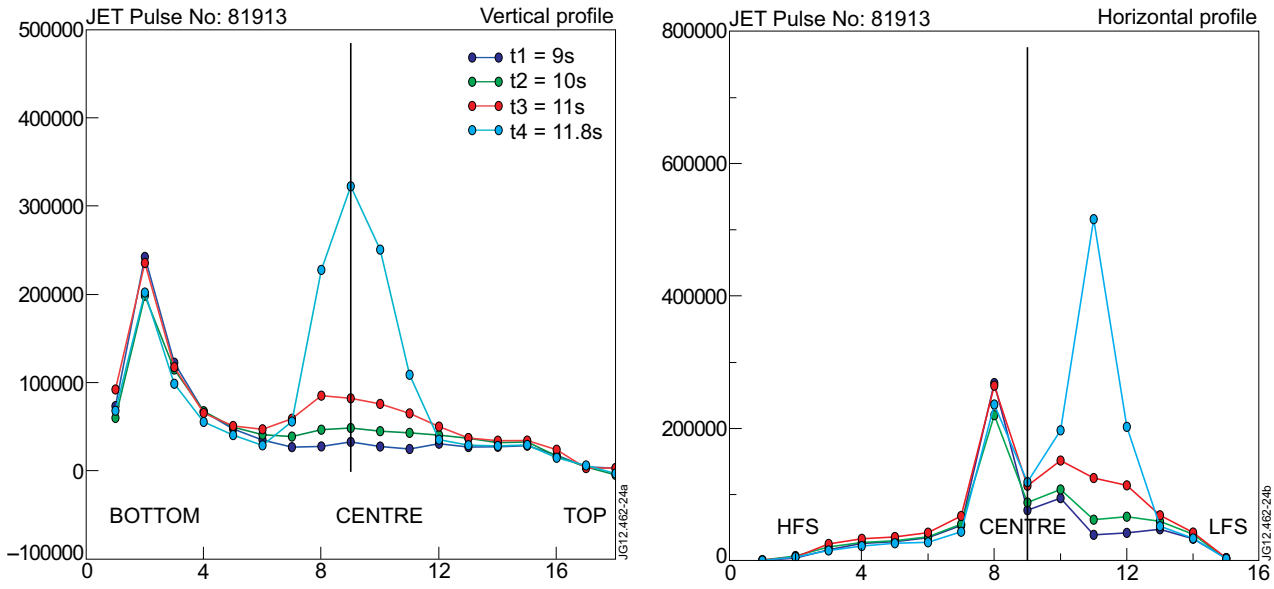

Figure 24: (left) vertical profile of radiated power for Pulse No: 91913 obtained from the horizontal lines of sight of the KB5 bolometer (plotted in figure 23). 4 times chosen during the Prad increase are represented (right) corresponding horizontal profile obtained with the vertical lines of sight of the KB5 bolometer.

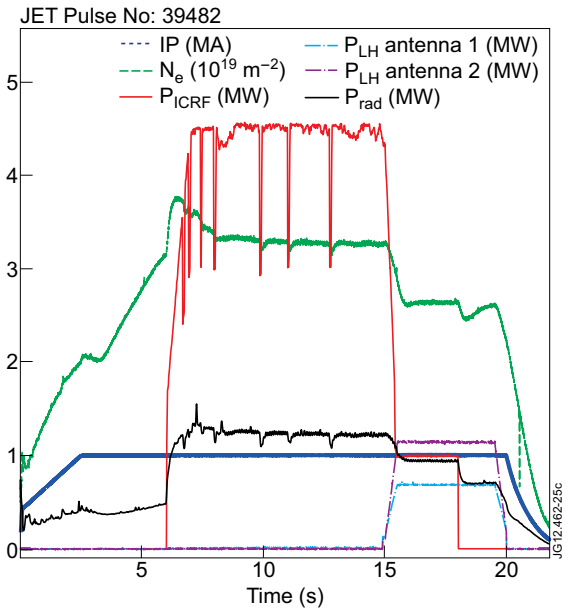

Figure 25: Scenario of Pulse No: 39482 in Tore Supra.

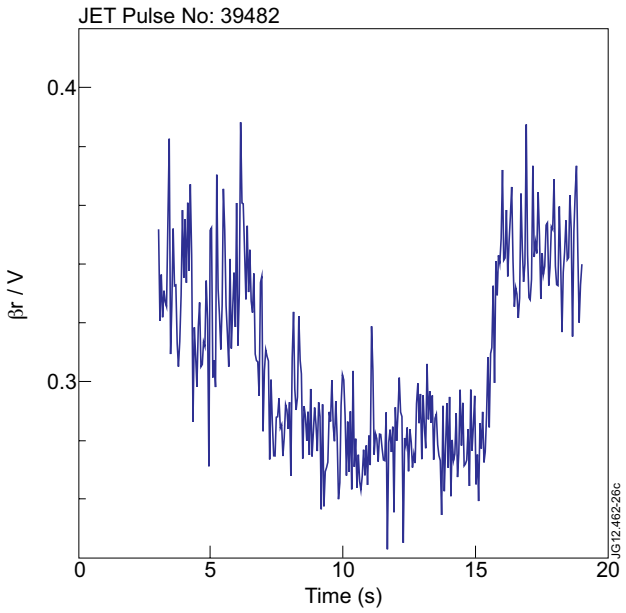

Figure 26: βr/V as a function of time for Pulse No: 39482 of TS.

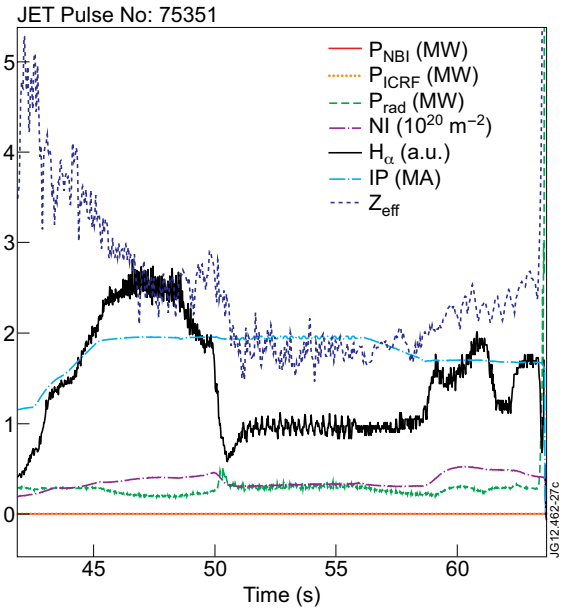

Figure 27: Scenario of Pulse No: 75351 in JET in Ohmic in Carbon environment. the limiter phase extends from 45 to 50s on the Ip plateau.

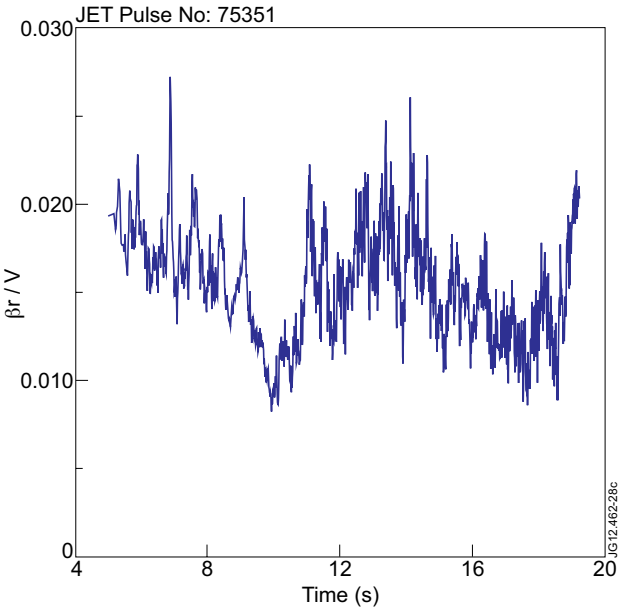

Figure 28: βr/V as a function of time for Pulse No: 75351 of JET, Ohmic shot in Carbon environment. Limiter Phase: 45-50s Divertor phase: >50s